Chapter 3

Crystal structure and catalytic mechanism of the LPS 3-O-deacylase PagL from *Pseudomonas aeruginosa*

Lucy Rutten*, Jeroen Geurtsen*, Wietske Lambert, Jeroen Smolenaers, Alexandre Bonvin, Alex de Haan, Peter van der Ley, Maarten Egmond, Piet Gros, and Jan Tommassen

***** L.R. and J.G. contributed equally to this work

Proc. Natl. Acad. Sci. U S A 103: 7071-7076, 2006

Abstract

Pathogenic Gram-negative bacteria can modify the lipid A portion of their lipopolysaccharide in response to environmental stimuli. 3-*O*-deacylation of lipid A by the outer membrane enzyme PagL modulates signalling through Toll-like receptor 4, leading to a reduced host immune response. We found that PagL is widely disseminated among Gram-negative bacteria. Only four residues are conserved: a Ser, His, Phe, and Asn residue. Here, we describe the crystal structure of PagL from *Pseudomonas aeruginosa* to 2.0-Å resolution. It consists of an eight-stranded β-barrel with the axis tilted by ~30° with respect to the lipid bilayer. The structure reveals that PagL contains an active-site with a Ser-His-Glu catalytic triad and an oxyanion hole that comprises the conserved Asn. The importance of active-site residues was confirmed in mutagenesis studies. Although PagL is most likely active as a monomer, its active-site architecture shows high resemblance to that of the dimeric 12-stranded outer membrane phospholipase A. Modelling of the substrate lipid X onto the active-site reveals that the 3-*O*-acyl chain is accommodated in a hydrophobic groove perpendicular to the membrane plane. In addition, an aspartate makes a hydrogen bond with the hydroxyl group of the 3-*O*-acyl chain, probably providing specificity of PagL toward lipid A.

Introduction

The outer membrane of Gram-negative bacteria functions as a permeability barrier that protects the bacteria against harmful compounds from the environment. It is an asymmetric bilayer with phospholipids and lipopolysaccharide (LPS) in the inner and outer leaflet, respectively. LPS contains three covalently linked domains: lipid A, the core, and the *O*-antigen (Raetz and Whitfield, 2002). Lipid A forms the hydrophobic membrane anchor and is responsible for the endotoxic activity of LPS. In *Escherichia coli*, it consists of a 1,4'-bisphosphorylated β-1,6-linked glucosamine disaccharide, which is substituted with *R*-3-hydroxymyristic acid (3OH C14) residues at positions 2, 3, 2', and 3' via ester or amide linkage. Secondary lauroyl and myristoyl groups substitute the hydroxyl group of 3OH C14 at the 2' and 3' positions, respectively. The underlying mechanism for LPS toxicity is its recognition by the host Toll-like receptor 4–MD2 complex, resulting in a signalling cascade within the host cell. Signalling eventually leads to activation of the transcription factor NF-κB, which regulates the production of pro-inflammatory cytokines (reviewed in Miyake, 2004).

Several Gram-negative bacteria, including *Salmonella enterica* serovar Typhimurium (*S.* Typhimurium), covalently modify their LPS in response to environmental stimuli. These modifications usually require the two-component regulatory system PhoP/PhoQ, which can be activated by antimicrobial peptides or repressed by high concentrations of divalent cations (Bader *et al.*, 2005). The PhoP/PhoQ system activates or represses the expression of >40 genes, some of which are involved in antimicrobial peptide resistance. Two integral outer membrane enzymes, the PhoP/PhoQ-activated gene products PagP and PagL, can alter the number of acyl chains in lipid A (reviewed in Trent, 2004). PagP is a palmitoyl transferase that transfers a palmitoyl moiety from a phospholipid to the *R*-3-hydroxyacyl chain at the 2 position of the glucosamine disaccharide of lipid A (Bishop *et al.*, 2000). PagL hydrolyses the ester bond at the 3 position of lipid A, thereby releasing the primary 3OH C14 moiety (Trent *et al.*, 2001). Both lipid A modifications reduce Toll-like receptor 4 signalling, which could help bacteria to evade the host immune system (Kawasaki *et al.*, 2004).

PagL was originally identified in *S.* typhimurium (Trent *et al.*, 2001). Recently, we identified PagL homologs in numerous other Gram-negative bacteria (Geurtsen *et al.*, 2005). Although the overall sequence conservation was rather low, the enzymatic activity of two of these homologs, including that of *Pseudomonas aeruginosa*, was confirmed because they deacylated *E. coli* LPS. Because *P. aeruginosa* lipid A carries 3OH C10, rather than 3OH C14 at the 3 position, these results also demonstrate that the enzyme lacks fatty acyl chain-length specificity. Furthermore, PagL was predicted to

form an eight-stranded β-barrel, and Ser-128 and His-126 of *P. aeruginosa* PagL were shown to be essential for activity (Geurtsen *et al.*, 2005). Here, we present the crystal structure of PagL from *P. aeruginosa* at 2.0-Å resolution and provide insights into the catalytic mechanism and substrate binding of the enzyme.

Materials and Methods

Site-directed mutagenesis

Mutations were introduced in *pagL* by using the QuikChange Site-Directed Mutagenesis kit (Stratagene) and the primers listed in Table 1. Plasmid $pPagL_{(Pa)}$ encoding wild-type PagL, including the signal sequence (Geurtsen *et al.*, 2005), was used as the template in which the mutations were created. The presence of the correct mutations was confirmed by nucleotide sequencing in both directions.

Construction of an *E. coli metE* mutant

The *metE* gene from *E. coli* strain AM1095 (Hoekstra *et al.*, 1976) was amplified by PCR. Chromosomal template DNA was prepared by resuspending ~10^9 bacteria in 50 ml of distilled water, after which the suspension was heated for 15 min at 95°C. The suspension was then centrifuged for 1 min at 16,100 x *g*, and the supernatant was used as template DNA. The sequence of the forward primer, including an ATG start codon, was 5'-AAATGACAATATTGAATCA-3'. The sequence of the reverse primer, which included a stop codon, was 5'-TTTTACCCCCGACGCAAGT-3'. The PCR was done under the following conditions: 50 ml total reaction volume, 25 pmol of each primer,

TABLE 1

Primers used for site-directed mutagenesis

Name[a]	Sequence (5'-3')[b]
D106A_FW	TCCCTGAACTTCGAAGCGCGCATCGGCGCCGGC
D106A_REV	GCCGGCGCCGATGCGCGCTTCGAAGTTCAGGGA
N129A_FW	GCGATCCACTATTCCGCGGCCGGCCTGAAACAG
N129A_REV	CTGTTTCAGGCCGGCCGCGGAATATGTGATCGC
N136A_FW	GGCCTGAAGTTCGCCGCGGGCCAGTCGGTCGGC
N136A_REV	GCCGACCGACTGGCCCGCGGCGAACTTCAGGCC
E140A_FW	CCGAACGACGGTATCGCGTCCTACAGCCTGTTC
E140A_REV	GAACAGGCTGTAGGACGCGATACCGTCGTTCGG

[a] The primer name gives the amino acid substitution, e.g., N136A_FW indicates that the oligonucleotide shown was used as the forward primer in a site-directed mutagenesis procedure to substitute the Asn at position 136 PagL by an alanine.
[b] Introduced mutations are underlined.

0.2 mM dNTPs, 3 nl of template DNA solution, 1.5% dimethyl sulfoxide, 1.75 units of Expand High Fidelity enzyme mix with buffer supplied by the manufacturer (Roche). The temperature program was as follows: 95°C for 3 min, 30 cycles of 1 min at 95°C, 1 min at 60°C, and 3 min at 72°C, followed by 10 min at 72°C and subsequent cooling to 4°C. The PCR product was purified from agarose gel and subsequently cloned into pCRII-TOPO. The resulting plasmid, designated pMetE, was partially digested with MluI and then ligated with the 801-bp MluI fragment of pBSL141 (Alexeyev and Shokolenko, 1995) harbouring a gentamicin (Gm)-resistance cassette. The ligation-mixture was used to transform *E. coli* DH5α using the $CaCl_2$ method (Sambrook *et al.*, 1989). A plasmid with the correct restriction digestion profile was designated pMetE::Gm^R, and harboured the *metE* gene with a inserted Gm-resistance gene in the same orientation as the *metE* gene itself. A methionine-auxotrophic derivative of AM1095 was constructed by marker exchange. Strain AM1095 was transformed with 6 µg of the 3-kb EcoRI fragment, containing the *metE* gene with the inserted Gm^R cassette from pMetE::Gm^R. Colonies were selected on LB agar plates containing 1 µg/ml Gm. Gm^R transformants were tested for methionine auxotrophy by growing on minimal medium plates in the absence or presence of 20 µg/ml methionine, and a methionine-auxotroph was designated JG201. Strain JG301, a methionine-auxotrophic derivative *E. coli* BL21 Star (DE3) (Invitrogen), was subsequently obtained by P1 transduction, using strain JG201 as the donor.

Production of PagL

To induce expression of PagL without its signal sequence, *E. coli* BL21 Star (DE3) (Invitrogen) containing pPagL(-) (Geurtsen *et al.*, 2005) was grown in LB broth until mid-exponential phase. Expression of the *pagL* gene was then induced by adding 1 mM isopropyl-1-thio-b-D-galactopyranoside (IPTG), after which incubation at 37°C was continued. To obtain PagL containing selenomethionine (Se-Met), *E. coli* strain JG301 (see above) transformed with pPagL(-) was grown in minimal medium (Winkler and de Haan, 1948) supplemented with 0.5% glucose and 50 µg/ml Se-Met. Inclusion bodies, containing PagL, were isolated as described (Dekker *et al.*, 1995), with some adaptations, i.e., centrifugation steps to collect the inclusion bodies were prolonged to 2 h. Inclusion bodies were solubilised in 8 M urea/10 mM glycine (pH 8.0) to a protein concentration of ~10 mg/ml. The urea-solubilised PagL was centrifuged at 150,000 ×*g* for 1 h to remove insoluble material. To remove residual non-protein contaminants, four volumes of 20% (wt/vol) trichloroacetic acid were added. Precipitated proteins were collected by centrifugation and washed with water in three rounds of resuspending and centrifuging. The protein pellet was then solubilised in 8 M urea/10 mM glycine (pH 8.0).

In vitro folding and purification of PagL

PagL was folded *in vitro* by 2-fold dilution from a stock solution in 8 M urea into 10% (wt/vol) lauryldimethylamine-oxide, followed by 10 min of sonication using a Branson 1210 Sonifier. Refolded PagL was diluted 3- to 4-fold with buffer A [20 mM Tris·HCl, pH 8.5/0.08% (wt/vol) pentaethyleneglycol monodecyl ether ($C_{10}E_5$)] and purified by fast-protein liquid chromatography (FPLC) using a 1-ml monoQ ion-exchange column (Amersham Pharmacia) that was pre-equilibrated with buffer A. PagL was eluted with a linear gradient of 0–1 M NaCl in buffer A. Fractions containing PagL were pooled and concentrated to ~10 mg/ml by using Centricon concentrators with a molecular mass cut-off of 3 kDa (Amicon). The protein was then dialysed three times overnight against 10 ml of 2 mM Tris·HCl, pH 8.5/0.06% $C_{10}E_5$ (vol/vol) using a membrane with a molecular mass cut-off of 3.5 kDa.

Crystallisation and structure determination

PagL was crystallised by using the hanging-drop vapour diffusion method. Crystals grew in the C2 space group, using a condition containing 3% PEG3000/25% glycerol/10 mM calcium acetate/0.1 M Tris-HCl, pH 8.5 at 20°C. Se-Met PagL crystals were grown in the same condition, with 1 mM DTT added to the protein solution. Crystals were harvested from the drops with a cryo-loop and directly cooled into liquid nitrogen. Data sets were obtained at 100 K on a charge-coupled device detector at beam line ID14-EH4 at the European Synchrotron Radiation Facility. Native data were collected to 2.0-Å resolution. Data of the Se-Met PagL crystal was collected at λ_{peak} = 0.9795 to 2.8-Å resolution. All data were indexed and processed by using DENZO and SCALEPACK (Otwinowski and Minor, 1997). Table 2 summarises data collection information. The structure of PagL was solved by using a combination of Se-Met single-wavelength anomalous dispersion (SAD) and molecular replacement (MR). From the Se-Met SAD data set, the two selenium atoms in the asymmetric unit (one per PagL molecule) were located by using standard programs (Storoni *et al.*, 2004; Weeks and Miller, 1999; Schneider and Sheldrick, 2002). Unfortunately, the anomalous signal was too low to obtain an interpretable density-modified electron-density map. Therefore, we attempted MR. Whereas all commonly used MR programs failed, the program PHASER (Storoni *et al.*, 2004) provided an MR solution using a polyalanine β-barrel model of the NspA structure, lacking the loops. The poor phases obtained from the incomplete model were sharpened by using the prime-and-switch algorithm in the program SOLVE (Storoni *et al.*, 2004). The positions of the seleniums indicated the locations of the methionines, which enabled us to correctly build a few β-strands by using the program

O (Jones *et al.*, 1991). Subsequently, the complete model could be built automatically by using ARP/WARP (Perrakis *et al.*, 2001), which was not the case directly after MR. The structure was refined by using REFMAC 5.0 (Winn *et al.*, 2001), using TLS groups for the separate molecules in the asymmetric unit. Refinement statistics are summarised in Table 2, and the electron density map is shown in Fig. 1.

TABLE 2

Data collection and refinement statistics

	Native	Se-Met
Data collection		
Space group	C2	C2
Cell dimensions		
a(Å)	92.26	93.21
b(Å)	48.99	47.66
c(Å)	105.03	103.45
β(°)	115.46	113.39
Resolution , Å (outer shell)	2.00(2.05)	2.80(2.87)
R_{sym} or R_{merge}	0.051(0.380)	0.098(0.515)
$I / \sigma I$	20.9(3.0)	19.3(3.4)
Completeness (%)	90.3(52.2)	99.8(97.6)
Redundancy	3.1(2.7)	6.8(6.9)
Refinement		
Resolution (Å)	2.00	
No. of reflections	26283	
R_{work} / R_{free}	0.198 / 0.233	
No. of atoms	2518	
Protein	2	
Ligand/ion	12 ($C_{10}E_5$ parts) / 1 (Ca^{2+})	
Water	121	
B-factors		
Protein	29.40	
ligand/ion	50.22 / 22.41	
Water	39.97	
rms deviations		
Bond lengths (Å)	0.017	
Bond angles (°)	1.657	

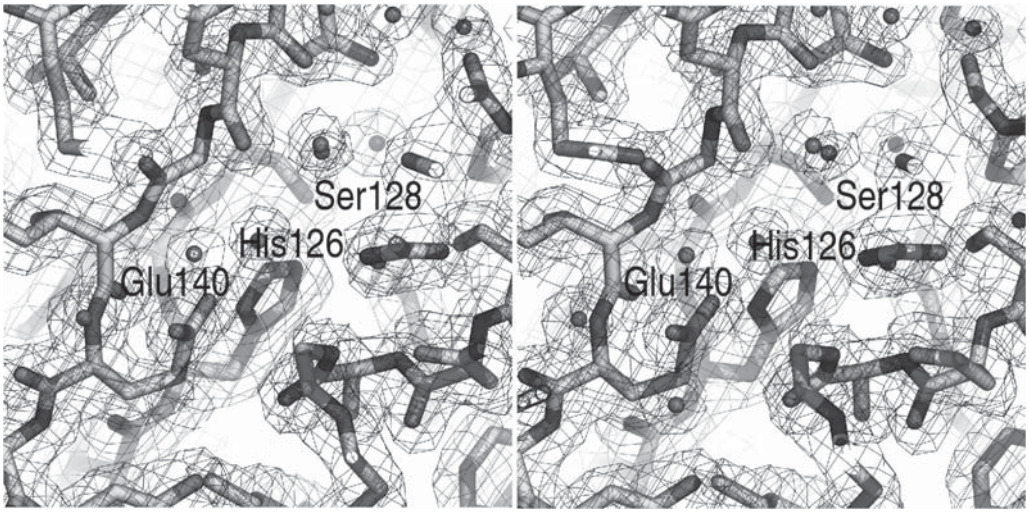

Fig. 1. Stereoview of the catalytic site with the final $2F_o$-F_c electron density map, at 2.0 Å resolution and contoured at 1σ, shown as chicken wire. Protein is shown as sticks. Carbon atoms are shown in yellow, oxygen in red and nitrogen in blue. Catalytic triad residues are labelled.

Modelling of lipid X onto the active-site of PagL

Models of lipid X docked onto PagL were created by using the program HADDOCK (Dominguez *et al.*, 2003). The coordinates of PagL were taken from chain A of the structure and the lipid X coordinates were based on those of the LPS molecule that was co-crystallised with FhuA (Ferguson *et al.*, 1998). Ambiguous interaction restraints (AIRs) were defined, based on the information on the reaction mechanism: 3-Å-distance restraints were defined between the Ser-128 oxygen of PagL and the carboxyl carbon of lipid X and between the His-126 nitrogen (Nε2) and the ester oxygen of lipid X. Additional AIRs were imposed merely to ensure that the lipid X acyl chains were positioned at least as close to the PagL molecule as they could be in the outer leaflet of the outer membrane. First, an ensemble of 20 conformations of lipid X was generated by simulated annealing and molecular dynamics refinement in DMSO, which was subsequently used to generate 1,000 rigid body docking solutions. The best 200 solutions based on their intermolecular energy (sum of van der Waals, electrostatic, and AIR energies) were then submitted to a semiflexible refinement, during which lipid X was treated as fully flexible, whereas PagL could only move at defined flexible regions (side chains first, subsequently both side chains and backbone). All 200 models were finally refined in explicit solvent (DMSO was used to mimic the hydrophobic environment imposed by the membrane) and clustered based on root mean square deviation criteria.

The lowest energy structure from the lowest energy cluster was taken as best solution.

PagL assays

PagL activity was measured *in vivo* and *in vitro*. In the *in vivo* assay, exponentially growing cultures of *E. coli* BL21 Star (DE3) containing $pPagL_{(Pa)}$ or its mutant derivatives were induced by adding 1 mM IPTG (end concentration). After 75-min further incubation at 37°C, deacylation of the endogenous LPS was monitored by the analysis of whole-cell samples in Tricine-SDS/PAGE (Lesse *et al.*, 1990) and staining of the LPS with silver (Tsai and Frasch, 1982). For the quantitative *in vitro* assay, cell envelopes of the *E. coli* strains expressing wild-type or mutant PagL proteins, induced as described above, were isolated as described (Geurtsen *et al.*, 2005). The protein content of the cell envelopes was determined by using the Pierce BCA protein assay after boiling the samples in 0.1% SDS. The amount of native PagL in the cell envelopes was estimated by comparison of the band intensities with a dilution series of purified refolded PagL on a blot of an SDS/PAGE gel, which was stained with Ponceau. For all PagL variants, the concentration was between 70 and 90 mg per mg total cell envelope protein. PagL activity was determined by incubating cell envelopes (444 total protein content per ml) with *Neisseria meningitidis* L3 LPS as described (Bos *et al.*, 2004). The amount of 3OH C12 released in time was determined by gas chromatography using 2OH C12 as an internal standard as described (Patterson *et al.*, 1999). The *in vitro* assay was also used to determine the activity of *in vitro*-folded PagL. Apart from the release of 3OH C12 in time, the deacylation of the LPS was also verified by Tricine-SDS/PAGE and ESI/MS (Geurtsen *et al.*, 2005).

Results

Production, folding, and activity of recombinant PagL

PagL from *P. aeruginosa* was refolded from inclusion bodies. Folding could be monitored by SDS/PAGE analysis. Like many outer membrane proteins (OMPs), PagL showed heat modifiability (Fig. 2A). Usually, the folded form of an OMP has a higher electrophoretic mobility than its denatured form. In the case of PagL, however, the folded protein has a lower electrophoretic mobility as has been observed also for a few other small OMPs, i.e., OmpA171t, OmpX, and NspA (Pautsch *et al.*, 1999; Vandeputte-Rutten *et al.*, 2003). The same mobility shift was observed on Western blot for wild-type PagL folded *in vivo* (data not shown). Folded PagL was insensitive to denaturation by SDS, as it remained folded even in the presence of 2% SDS when not heated (Fig. 2A).

To verify that PagL was correctly folded *in vitro*, it was incubated with purified LPS of *N. meningitidis*. The LPS was converted into a form with a higher electrophoretic mobility (Fig. 2B), in agreement with the expected hydrolysis of the primary acyl chain at the 3 position of lipid A, which is 3OH C12 in the case of *N. meningitidis*. Deacylation of the LPS was confirmed by electrospray ionisation mass spectrometry (Fig. 3). The reaction was independent of the presence of divalent cations, as deacylation of LPS was still observed in the presence of 5 mM EDTA (Fig. 2B). Quantification of the amount of 3OH C12 released in time revealed a specific activity of 0.40 nmol 3OH C12 released per min per nmol of *in vitro* folded PagL. *E. coli* membranes containing overexpressed *in vivo* folded wild-type PagL displayed a lipid A-deacylase activity of ~0.22 nmol/min per nmol of PagL, which is comparable to the specific activity of *in vitro* folded PagL. We concluded that PagL was correctly folded *in vitro* into its active conformation and, thus, suitable for structure determination.

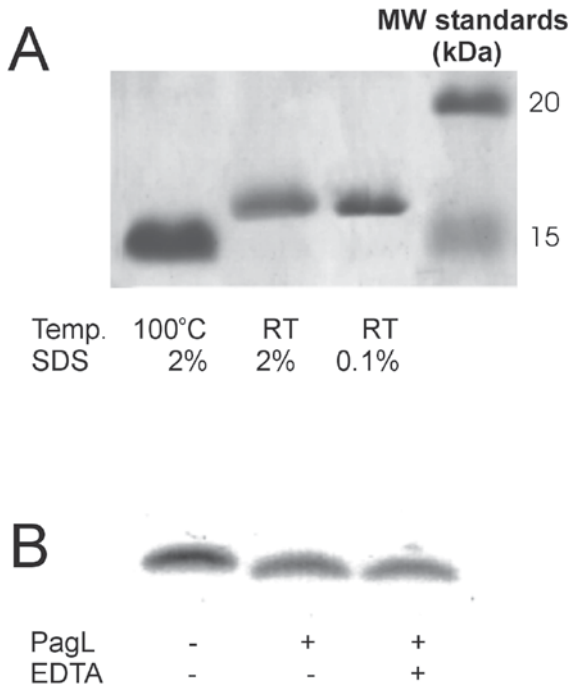

Fig. 2. Folding and *in vitro* activity of recombinant PagL. (A) Coomassie-stained SDS/PAGE gel showing the heat modifiability of purified, refolded PagL. Samples were treated in sample buffer containing either 2% or 0.1% SDS and at room temperature (RT) or 100°C before electrophoresis. The positions of molecular mass standard proteins are shown at the right. (B) Purified *N. meningitidis* LPS was incubated in a detergent-containing buffer with or without refolded PagL and analysed by Tricine-SDS/PAGE and staining with silver.

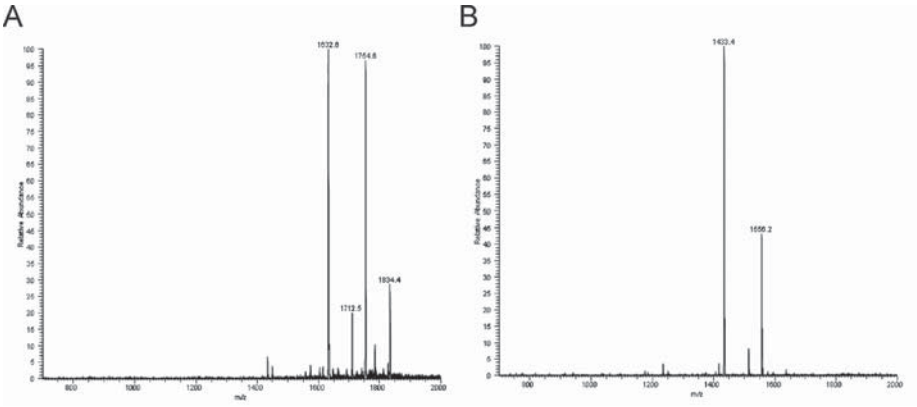

Fig. 3. Structural analysis by ESI/MS of wild-type and *in vitro* PagL-modified *N. meningitidis* L3 LPS. Lipid A moieties of wild-type (A) and *in vitro* PagL-modified (B) *N. meningitidis* L3 LPS were analysed by ESI/MS as described (Geurtsen *et al.*, 2005). Major peaks at *m*/*z* 1713, 1834, 1556, and 1433 were interpreted as the characteristic hexaacylated *bis*-phosphate species that is typically found in *N. meningitidis*, a hexaacylated *bis*-phosphate species substituted with a phosphoethanolamine, a 3-*O*-deacylated *mono*-phosphate species substituted with a phosphoethanolamine, and a 3-*O*-deacylated *mono*-phosphate species, respectively. The major peaks at *m*/*z* 1632 and 1754 probably represent fragment ions of the species at *m*/*z* 1713 and 1834.

Structure determination of PagL

PagL was crystallised in the C2 space group, containing two molecules in the asymmetric unit (Fig. 4). The structure of PagL was solved with a combination of MR using the program PHASER (Storoni *et al.*, 2004), together with single-wavelength anomalous dispersion. MR was successfully performed by using a polyalanine model of the β-stranded part of NspA. The calculated $2F_o - F_c$ maps (even after prime-and-switch in RESOLVE (Terwilliger, 2003) did not allow for initial model tracing by hand or by automated model building with ARP/wARP (Perrakis *et al.*, 1997). Determination of the position of the single methionine present in PagL, using the anomalous signal of the selenium from a crystal of Se-Met-substituted protein, enabled limited model tracing and subsequent automated model building. The structure was refined to 2.0-Å resolution.

The overall structure of PagL consists of an eight-stranded anti-parallel β-barrel, which is consistent with our earlier prediction of its topology (Geurtsen *et al.*, 2005). So far, the N and C termini of the β-barrel part in all OMP structures solved are facing the periplasm (reviewed in Schulz, 2000). Therefore, we propose that the same holds for PagL. In this orientation, the previously identified active-site residues Ser-128 and His-126 (Geurtsen *et al.*, 2005) are located near the hydrophilic/hydrophobic boundary of the outer leaflet of the outer membrane (Fig. 5A). This position would be consistent with the location of the scissile bond of the substrate LPS. Like other OMPs, PagL has long extracellular loops (L) and short periplasmic turns (T), except for T1, which is exceptionally long (Fig. 5A).

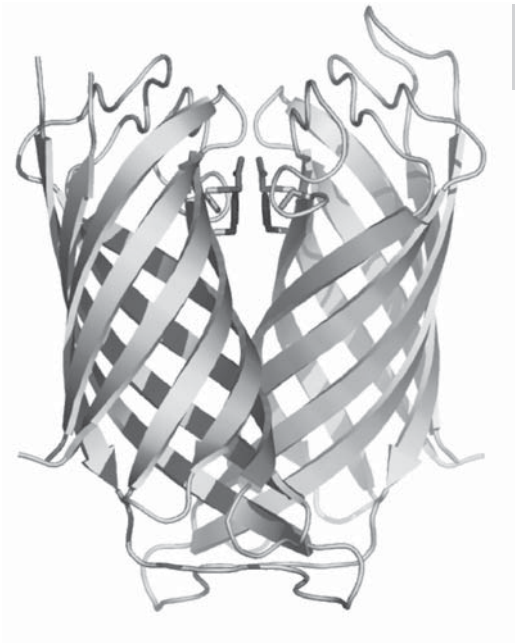

Fig. 4. PagL dimer in the crystal structure. The active-site residues Ser-128, His-126, and Glu-140 are coloured pink, blue, and red, respectively.

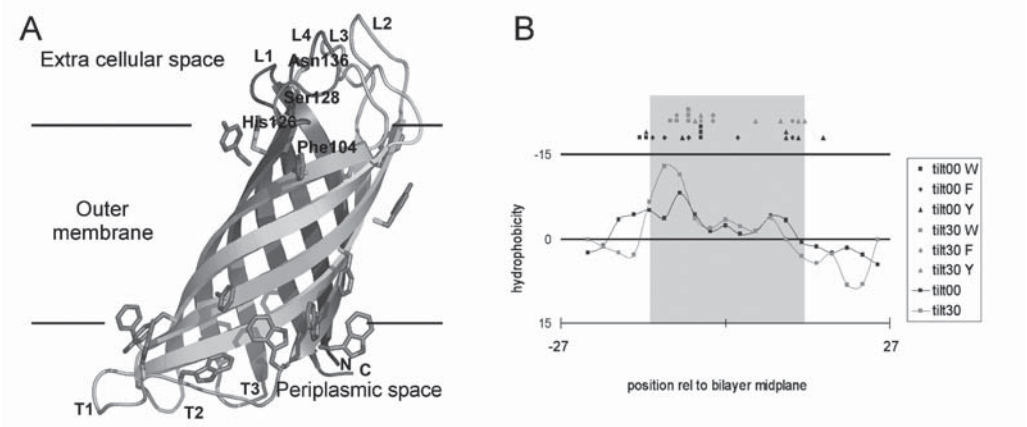

Fig. 5. PagL structure and membrane orientation. (A) Ribbon representation of PagL. The N and C termini are labelled and coloured blue and red, respectively, with gradient colours in between. The four extracellular loops are labelled L1–L4, and the three periplasmic turns are labelled T1–T3. Aromatic residues located at the presumed membrane boundaries are shown in gray, with nitrogen and oxygen atoms shown in blue and red, respectively. The only four completely conserved residues among PagL homologs are labelled. (B) Hydrophobicity profiles for the outward-facing PagL residues as a function of membrane position (periplasmic side left, extracellular side right) are shown as solid lines. Negative $\Sigma(\Delta G)$ values indicate regions that are more hydrophobic. The blue line and symbols present results for the positions with the β-barrel axis aligned along the membrane normal, whereas the magenta line and symbols are for the protein tilted by 30°. The symbols represent the $C\gamma$ positions of Trp (squares), Tyr (circles), and Phe (triangles) residues that form the inner and outer aromatic girdles. The image shown in (A) was prepared with PYMOL (www.pymol.org).

Orientation of PagL in the membrane

Like most other OMPs, PagL contains two girdles of aromatic residues, which are located at the hydrophobic/hydrophilic boundaries of the membrane and are assumed to stabilise the position of the protein in the membrane. Because these girdles are not perpendicular to the β-barrel axis of PagL, as they usually are in OMPs, the orientation of PagL in the membrane may be tilted (Fig. 5A). Therefore, we calculated the net hydrophobicity at the β-barrel surface as a function of the height in the membrane as described (Wimley, 2002); this was done for two orientations, i.e., with the β-barrel axis parallel or with a 30° tilt angle relative to the membrane normal (Fig. 5B). In the tilted orientation, the graph resembles the average graph calculated for all OMP β-barrel structures, in which two hydrophobic peaks represent the aromatic girdles (Wimley, 2002). Remarkably, the hydrophobic peak at the extracellular side is much lower than that at the periplasmic side, which can easily be explained by the presence of a highly hydrophilic active-site at that height in the barrel (see below). Also, in the parallel orientation, two hydrophobic peaks can be discriminated. However, the area of hydrophobicity of the intracellular peak extends considerably into the periplasm, suggesting that a parallel orientation is energetically highly unfavourable. Therefore, we propose that PagL has a tilted orientation in the membrane.

PagL catalytic-mechanism

Previously, we identified PagL homologs in the genomes of a wide variety of Gram-negative bacteria (Geurtsen *et al.*, 2005). These homologs exhibited a low overall mutual sequence identity, with only 10 conserved residues among 14 different homologs. Here, we performed a more extensive search, which revealed additional PagL homologs in *Caulobacter crescentus*, *Collimonas fungivorans*, *Chlorobium tepidum*, *Rhodospirillum rubrum*, *Sinorhizobium meliloti*, and *Ralstonia eutropha*. An alignment of all currently identified PagL homologs is presented in Fig. 6. Among all PagL homologs identified so far, only four amino acid residues are fully conserved, i.e., Phe-104, His-126, Ser-128, and Asn-136 of the *P. aeruginosa* PagL sequence.

Active sites of hydrolases comprise three important regions: the catalytic site, a substrate-binding site, and an oxyanion hole. Classical serine esterases contain a catalytic site consisting of a Ser-His-Asp/Glu triad. The histidine abstracts a proton from the serine residue, after which the serine performs a nucleophilic attack on the carbonyl carbon of the scissile bond. This attack can only be performed efficiently if the Nε2 of the histidine is deprotonated. Deprotonation of the histidine is achieved by stabilisation of the proton on the Nδ1 of the histidine via a hydrogen bond with an acidic residue.

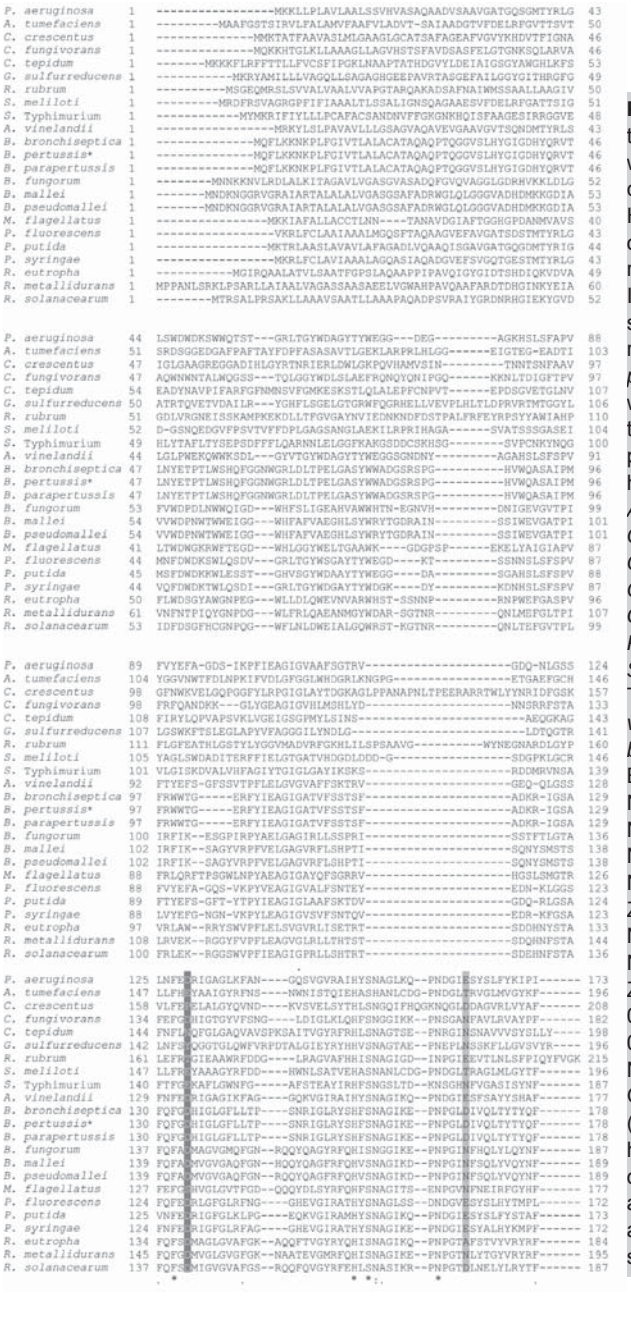

Fig. 6. Multiple sequence alignment of the precursor PagL proteins. Sequences were aligned using CLUSTALW (www.ch.embnet.org/software/ClustalW.html). Hyphens indicate gaps introduced for optimal alignment. Absolutely conserved residues are marked with asterisks. Indicated by colons and dots are strongly and weakly conserved residues, respectively. The *pagL* ORF in *Bordetella pertussis* is disrupted by a frame shift, which was restored for this alignment by adding two nucleotides in codon 33. The GenBank protein accession numbers for the PagL homologs are: *P. aeruginosa* NP_253350, *Agrobacterium tumefaciens* AAK87616, *Caulobacter crescentus* AAK25066, *Collimonas fungivorans* AAT42436, *Chlorobium tepidum* NP_663142, *Geobacter sulfurreducens* AE017180§, *Rhodospirillum rubrum* ZP_00270083, *Sinorhizobium meliloti* CAC46357, *S.* Typhimurium AAL21147, *Azotobacter vinelandii* ZP_00089534, *Bordetella bronchiseptica* NP_890306, *B. pertussis* BX470248§, *Bordetella parapertussis* NP_885487, *Burkholderia fungorum* NZ_AAAJ03000003§, *Burkholderia mallei* NC_002970§, *Burkholderia pseudomallei* NC_002930§, *Methylobacillus flagellatus* ZP_00564368, *Pseudomonas fluorescens* NZ_AAAT03000006§,*Pseudomonasputida* NC_002947§, *Pseudomonas syringae* ZP_00125465, *Ralstonia eutropha* ZP_00168928, *Ralstonia metallidurans* ZP_00274744, and *Ralstonia solanacearum* NP_522762. The symbol § indicates GenBank™ accession numbers of whole (unfinished) genomes, in which the PagL homologs were manually identified. The dark and light gray boxes indicate residues at the equivalent positions of Asp-106 and Glu-140 of the *P. aeruginosa* PagL sequence, respectively.

Usually, this acidic residue is an aspartate or a glutamate. However, in a few exceptions, such as in outer membrane phospholipase A (OMPLA) of *E. coli*, an asparagine residue is also able to stabilise the deprotonated state of the Nε2 of the histidine (Snijder *et al.*, 1999).

Site-directed mutagenesis studies have shown that His-126 and Ser-128 are important for catalytic activity and constitute part of the active-site of PagL (Geurtsen *et al.*, 2005). In the crystal structure, two acidic residues, Glu-140 and Asp-106, are located in close proximity to His-126. A hydrogen bond is present between the carboxylate of Glu-140 and the Nδ1 hydrogen of His-126, which implies that Glu-140 is the acidic component of the catalytic triad. This notion is supported by the observation that a Glu140Ala substitution reduced the activity of PagL *in vivo* in *E. coli* membranes (Fig. 7). LPS was almost completely converted into its 3-*O*-deacylated form 75 min after induction of expression of wild-type *pagL*, whereas ~50% remained in the acylated form when the mutant PagL was produced. In the quantitative assay, in which the release of 3OH C12 from exogenously added Neisserial LPS is measured, the mutated protein appeared 142-fold less active than the wild type.

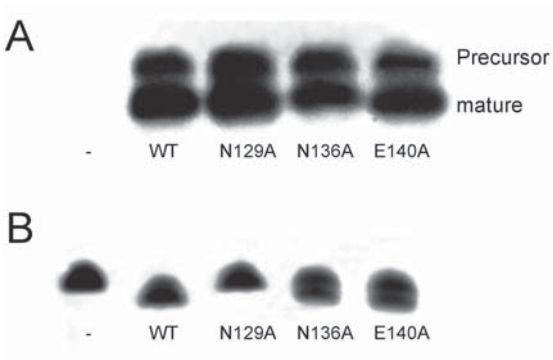

Fig. 7. Identification of residues important for PagL activity. Cells of *E. coli* BL21 Star (DE3) containing the empty pET11a vector, the $pPagL_{(Pa)}$ plasmid, or the mutant $pPagL_{(Pa)}$ plasmids, exponentially growing in LB, were induced with isopropyl-β-D-thiogalactoside for 75 min, after which 1-A_{600}-unit culture samples were collected and analysed by SDS/PAGE followed by immunoblotting with primary antibodies against PagL (A) and by Tricine-SDS/PAGE to visualise LPS (B). In *A*, the positions of mature PagL and of the precursor form, which accumulated because of overexpression, are indicated.

Another acidic residue, Asp-106, is present on the opposite side of His-126. In the crystal structure, Asp-106 coordinates a Ca^{2+} ion. Because PagL activity is not influenced by EDTA, this Ca^{2+} ion is likely not relevant for activity and may just be a crystallisation artefact. Because Asp-106 points toward the hydrophobic region of the membrane, which is not a favourable position for a charged residue, it seems plausible that it has an important function in the catalytic mechanism. To test this possibility, we substituted Asp-106 by Ala. Unfortunately, the mutant protein was poorly expressed (data not shown), indicating that the substitution caused folding and/or stability problems of the protein.

To gain further insight into the catalytic mechanism, we modelled lipid X, the smallest known substrate of PagL *in vitro* (Trent *et al.*, 2001) onto the active-site of PagL by using the program HADDOCK (Dominguez *et al.*, 2003). Several restraints were used. The distances between the hydroxyl oxygen of Ser-128 and the carbonyl carbon of the scissile bond and between the Nε2 of His-126 and the main-chain oxygen of the ester bond were both restrained to 3 Å. Furthermore, the acyl chains of lipid X were restrained to point towards the periplasm. In the resulting model (Fig. 8), the residual acyl chain (i.e., the chain to be cleaved off from the substrate) of lipid X is bound in a well defined hydrophobic groove, whereas the acyl chain of the leaving group is loosely bound into a second hydrophobic groove. The conserved residue Phe-104, which makes a hydrophobic interaction with the residual acyl chain, is likely to be a key residue for positioning the substrate into the correct orientation. Furthermore, the hydroxyl group of the residual acyl chain makes a hydrogen bond to Asp-106, suggesting a possible role for this residue in substrate specificity.

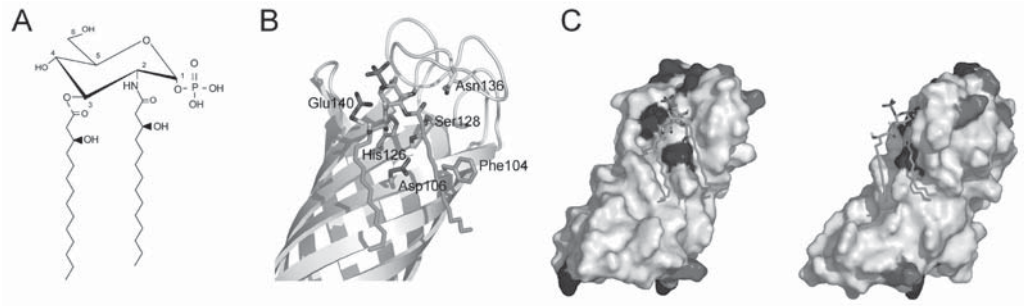

Fig. 8. Modelling of lipid X onto the active site of PagL. (A) Schematic representation of lipid X. (B) Lipid X modelled onto the active site of PagL. PagL is represented as a gray ribbon diagram. Lipid X is shown as green sticks with oxygen atoms in red and a phosphate atom in magenta. The hydrogen atoms from hydroxyl groups are shown in gray. Some amino acid residues important for PagL activity are shown as sticks and are labelled. (C) Two views (~90° rotated) of the electrostatic surface potential of PagL with lipid X. Positively and negatively charged residues are coloured blue and red, respectively. Lipid X is shown as green sticks. The images in *B* and *C* were prepared with PYMOL (www.pymol.org).

The structure of one other outer membrane esterase has been solved, i.e., that of OMPLA, which forms a 12-stranded β-barrel with a catalytic site composed of a Ser-His-Asn catalytic triad (Dominguez *et al.*, 2003). To compare the catalytic sites of OMPLA and PagL, we superposed Ser-128 and His-126 of PagL onto Ser-144 and His-142 of OMPLA (Fig. 9). In both PagL and OMPLA, the active sites are located at comparable heights in the barrel relative to the membrane. Furthermore, Glu-140 of PagL occupies the structurally equivalent position of Asn-156, the acidic residue in the catalytic triad of OMPLA, consistent with Glu-140 being the acidic residue of the PagL catalytic triad. In

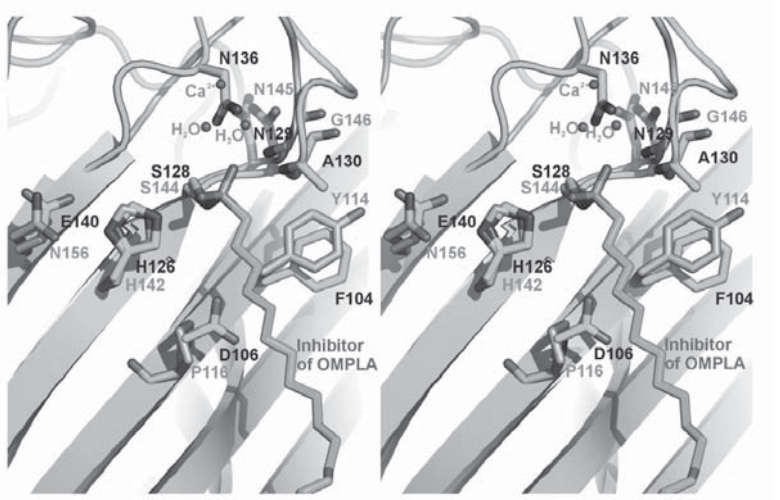

Fig. 9. Stereo diagram of the active site Ser-128 and His-126 of PagL superposed on the active site Ser-144 and His-142 of OMPLA. PagL is shown in cyan, whereas OMPLA is represented in orange. Residues and atoms that may have an important role for activity are shown as sticks and are labelled with cyan and orange text for PagL and OMPLA, respectively. The hexadecanesulfonyl moiety of an OMPLA inhibitor is covalently attached to Ser-144 of OMPLA and coloured green. The image was prepared by using PYMOL (www.pymol.org).

many serine hydrolases, the oxyanion hole consist of two backbone amide groups that form a slightly positively charged centre that stabilises the transient negative charge on the carbonyl oxygen of the substrate during the reaction. The oxyanion hole of OMPLA is formed by two backbone nitrogens from two glycine residues and two water molecules, coordinated by a calcium ion (Snijder *et al.*, 1999). For PagL, the oxyanion hole could well be formed by the two backbone nitrogens of the highly conserved Ala-130 and Gly-131 residues, which are located at the equivalent positions of the oxyanion-hole glycines in OMPLA. Comparison of the OMPLA and PagL active sites further showed that the side-chain nitrogen of Asn-136, the fourth completely conserved residue among the PagL homologs, occupies the position of one of the oxyanion-hole waters in OMPLA (Fig. 9). Therefore, we speculate that the side-chain amide group of Asn-136 is part of the oxyanion hole of PagL. This possibility is supported by the observation that an Asn136Ala mutant derivative of PagL was less active *in vivo* than wild-type PagL (Fig. 7). In the quantitative assay, the activity of this mutant protein was reduced 304-fold. In addition to the three highly or even completely conserved residues Ala-130, Gly-131, and Asn-136, which we postulate to form the oxyanion hole of PagL, one other residue, Asn-129, shows a high conservation among the PagL homologs (Fig. 6). Furthermore, the same residue is present at the equivalent position in OMPLA (Fig. 9). We propose that Asn-129 of PagL might play a crucial role in stabilising the conformation of loop 4

and thereby that of the oxyanion hole and the active-site. The importance of Asn-129 for the enzymatic activity is supported by the observation that an Asn129Ala mutant derivative of PagL showed no activity *in vivo* (Fig. 7), nor in the quantitative assay even after 27 h incubation with the substrate.

Discussion

The lipid A deacylase PagL was initially discovered in *S.* Typhimurium, and, recently, PagL homologs were identified in a wide variety of Gram-negative bacteria, including *P. aeruginosa*. By using these PagL homologs as leads, we were able to identify additional homologs, which now brings their total number to 23. Remarkably, besides the previously identified active-site His and Ser residues, only a Phe and an Asn residue are completely conserved among all homologs identified so far. Modelling with HADDOCK suggested that the phenylalanine is important for positioning the substrate correctly into a hydrophobic groove present on PagL, thereby bringing the scissile bond into close proximity to the active-site serine. This hypothesis is sustained by the presence of another aromatic residue, Tyr-114, at the equivalent position in OMPLA, which was shown to have similar active-site architecture. This tyrosine was shown to make a hydrophobic interaction in the crystal structure of OMPLA with the substrate analog hexadecanesulfonylfluoride. The close resemblance of the PagL active-site to that of OMPLA also allowed us to speculate about the location of the oxyanion hole and the possible role of the completely conserved asparagine (Asn-136) therein.

The catalytic triad of PagL is formed by His-126, Ser-128, and, most likely, Glu-140. The hypothesis that Glu-140, rather than Asp-106, is the third member of the catalytic triad is supported by several lines of evidence. First, Glu-140 is located at the structurally equivalent position of Asn-156, the postulated acidic residue in the catalytic triad of OMPLA. Second, Glu-140 forms a hydrogen bond with His-126. Third, mutagenesis showed that Glu-140 is important for PagL activity, although not essential, because residual activity was detected after its substitution by Ala. In OMPLA, Asn-156 is not essential either, because Asn156Ala substitution reduced OMPLA activity ~20-fold (Kingma *et al.*, 2000). A possible explanation is that OMPLA, and probably also PagL, has a highly functional oxyanion hole that can partly compensate for the loss of the acidic residue. The acidic residue of the catalytic triad of serine hydrolases can be formed by three different amino acids, i.e., Asp, Glu, and, more rarely, Asn. An alignment of all identified PagL homologs (Fig. 6) shows that always one of these residues is present at the position of Glu-140 in *P. aeruginosa* PagL, except in three cases, i.e., the PagL

homologs of *Agrobacterium tumefaciens*, *S. meliloti*, and *R. eutropha*, where a threonine, a threonine, and an alanine, respectively, are present. Theoretically, a threonine could take over the role of the acidic residue in forming a hydrogen bond with the active-site histidine, and it will be interesting to determine by site-directed mutagenesis and x-ray crystallography whether the threonine indeed plays such a role in the *A. tumefaciens* and *S. meliloti* enzymes. The *R. eutropha* enzyme may be less active, like the Glu140Ala-mutant derivative of *P. aeruginosa* PagL, and it will be interesting to determine whether its activity can be enhanced by substituting an acidic residue for the alanine. In the modelled PagL/lipid X structure, the hydroxyl group of the residual acyl chain makes a hydrogen bond to Asp-106. In OMPLA, a proline (Pro-116) is present at the equivalent position. It is tempting to speculate that Asp-106 determines the specificity of PagL for substrates with a hydroxyl group present at the correct position, i.e., for LPS. It will be interesting to determine the consequences of Asp106Pro and Pro116Asp substitutions in PagL and OMPLA, respectively, for the substrate specificity of the enzymes. It should be noted, however, that Asp-106 is not completely conserved among all PagL homologs, and one enzyme, i.e., that of *C. crescentus*, contains a proline at the equivalent position (Fig. 6).

Taken together, monomeric PagL has all features needed for activity, i.e., an active-site, an oxyanion hole, and a substrate-binding pocket within a single molecule. In contrast, OMPLA activity is activated *in vitro* by dimerisation (Snijder *et al.*, 1999). This raises the question in what way enzymatic activity of PagL is controlled. In *S.* Typhimurium, expression of *pagL* is under the control of the PhoP/PhoQ two-component regulatory system. However, silencing of PagL activity, when it is no longer beneficial to the bacterium, is not explained. A recent observation may provide an answer: PagL of *S.* Typhimurium is inhibited by modification of LPS with aminoarabinose (Kawasaki *et al.*, 2004). It was suggested that such modification might affect the membrane localisation or conformation of PagL. However, in *P. aeruginosa*, modification of LPS with aminoarabinose is found in combination with 3-*O*-deacylation of lipid A, suggesting that PagL activity is not regulated in this way in *P. aeruginosa* (Ernst *et al.*, 1999). In contrast to the activation caused by dimerisation of OMPLA, dimerisation of PagL could inhibit PagL activity. The active-sites of the two PagL molecules in the asymmetric unit are in close proximity (Fig. 4). It is tempting to speculate that this structure represents a dimeric state of PagL. After substitution of the active-site serine by a cysteine, we detected dimers of the protein when the membranes were analysed by SDS/PAGE in the absence of a reducing agent (data not shown), indicating that the active sites of the two PagL molecules could be very close *in vivo* as well. If indeed such a dimer is formed,

the active-site of one monomer is shielded for substrate binding by the other monomer. Therefore, dimerisation may be an inactivation mechanism for PagL, whereas it is an activation mechanism in the case of OMPLA.

Both the length of turn T1 and the position of the aromatic residues raised the idea that the PagL β-barrel is tilted relative to the membrane plane. Interestingly, such an assumption has been made for only one other OMP, i.e., the lipid A-modifying enzyme PagP (Ahn *et al.*, 2004). Analysis of the hydrophobic surface of the β-barrel indeed showed that a tilted orientation of PagL is more consistent with the average hydrophobicity profile of other β-barrels of known structure. The tilted orientation also explains why the periplasmic turn (T1) between strands 2 and 3 is asymmetrical and contains many aromatic residues. Considering the hydrophobicity profiles of possible orientations tested, a 30°-tilted orientation is expected to be energetically most favourable. However, in a biological membrane, there are many more forces and factors that determine the position of a protein. The shape of the LPS and phospholipids and the lateral pressure exerted by these will form a counterbalancing force against tilting of the barrel. Therefore, it cannot be concluded that PagL has a 30° tilt *in vivo*, although such an angle might be considered as the maximal possible tilt. Furthermore, control of the barrel tilt angle and, thereby, of the position of the active-site relative to the membrane might form another mechanism to control the enzymatic activity of PagL *in vivo*.

LPS is known for its endotoxic activity when administered to higher organisms. This endotoxic activity is responsible for the side effects that are often seen when vaccines that contain LPS are administered. LPS also has a powerful adjuvant activity. Unfortunately, a broad-scale use of this adjuvant quality is not possible because of the endotoxic activity. Recently, it has been shown that changing the physico-chemical properties of LPS influences its endotoxic activity (Raetz and Whitfield, 2002; Loppnow *et al.*, 1989; Steeghs *et al.*, 2002). Thus, LPS-modifying enzymes may be valuable tools for detoxification of LPS. We showed here that purified and *in vitro* refolded PagL is active against externally added LPS. Thus, *in vitro* refolded PagL might be used for the detoxification of LPS *in vitro* and thereby be useful for the development of new vaccines or adjuvants. Furthermore, the structure of PagL may form, especially because the active-site is on the outside of the barrel, a basis for the design of inhibitors with possible therapeutic value.

Acknowledgements

We are grateful for measurement time at the beam line ID14-EH4 at the European Synchrotron Radiation Facility in Grenoble. This work was supported by the council for Chemical Sciences of the Netherlands Organisation for Scientific Research (NWO-CW).

References

Ahn, V. E., Lo, E. I., Engel, C. K., Chen, L,, Hwang, P. M., Kay, L. E., Bishop, R. E., and Prive, G. G. (2004) A hydrocarbon ruler measures palmitate in the enzymatic acylation of endotoxin. *EMBO J.* **23:** 2931-2941.

Alexeyev, M. F., and Shokolenko, I. N. (1995) Mini-Tn10 transposon derivatives for insertion mutagenesis and gene delivery into the chromosome of gram-negative bacteria. *Gene* **160:** 59-62.

Bader, M. W., Sanowar, S., Daley, M. E., Schneider, A. R., Cho, U., Xu, W., Klevit, R. E., Le Moual, H., and Miller, S. I. (2005) Recognition of antimicrobial peptides by a bacterial sensor kinase. *Cell* **122:** 461-472.

Bishop, R. E., Gibbons, H. S., Guina, T., Trent, M. S., Miller, S. I., and Raetz, C. R. H. (2000) Transfer of palmitate from phospholipids to lipid A in outer membranes of Gram-negative bacteria. *EMBO J.* **19:** 5071-5080.

Bos, M. P., Tefsen, B., Geurtsen, J., and Tommassen, J. (2004) Identification of an outer membrane protein required for the transport of lipopolysaccharide to the bacterial cell surface. *Proc. Natl. Acad. Sci. U S A* **101:** 9417-9422.

Dekker, N., Merck, K., Tommassen, J., and Verheij, H. M. (1995) In vitro folding of *Escherichia coli* outer-membrane phospholipase A. *Eur. J. Biochem.* **232:** 214-219.

Dominguez, C., Boelens, R., and Bonvin, A. M. (2003) HADDOCK: a protein-protein docking approach based on biochemical or biophysical information. *J. Am. Chem. Soc.* **125:** 1731-1737.

Ernst, R. K., Yi, E. C., Guo, L., Lim, K. B., Burns, J. L., Hackett, M., and Miller, S. I. (1999) Specific lipopolysaccharide found in cystic fibrosis airway *Pseudomonas aeruginosa*. *Science* **286:** 1561-1565.

Ferguson, A. D., Hofmann, E., Coulton, J. W., Diederichs, K., and Welte, W. (1998) Siderophore-mediated iron transport: crystal structure of FhuA with bound lipopolysaccharide. *Science* **282:** 2215-2220.

Geurtsen, J., Steeghs, L., ten Hove, J., van der Ley, P., and Tommassen, J. (2005) Dissemination of lipid A deacylases (*pagL*) among gram-negative bacteria: identification of active-site histidine and serine residues. *J. Biol. Chem.* **280:** 8248-8259.

Hoekstra, W. P., de Haan, P. G., Bergmans, J. E., and Zuidweg, E. M. (1976) Transformation in *E. coli* K12: relation of linkage to distance between markers. *Mol. Gen. Genet.* **145:** 109-110.

Jones, T. A., Zou, J. Y., Cowan, S. W., and Kjeldgaard, M. (1991) Improved methods for building protein models in electron density maps and the location of errors in these models. *Acta. Crystallogr. A* **47:** 110-119.

Kawasaki, K., Ernst, R. K., and Miller, S. I. (2004) Deacylation and palmitoylation of lipid A by *Salmonellae* outer membrane enzymes modulate host signaling through Toll-like receptor 4. *J. Endotoxin Res.* **10:** 439-444.

Kawasaki, K., Ernst, R. K., and Miller, S. I. (2005) Inhibition of *Salmonella enterica* serovar Typhimurium lipopolysaccharide deacylation by aminoarabinose membrane modification. *J. Bacteriol.* **187:** 2448-2457.

Kingma, R. L., Fragiathaki, M., Snijder, H. J., Dijkstra, B. W., Verheij, H. M., Dekker, N., and Egmond, M. R. (2000) Unusual catalytic triad of *Escherichia coli* outer membrane phospholipase A. *Biochemistry* **39:** 10017-10022.

Lesse, A. J., Campagnari, A. A., Bittner, W. E., and Apicella, M. A. (1990) Increased resolution of lipopolysaccharides and lipooligosaccharides utilizing tricine-sodium dodecyl sulfate-polyacrylamide gel electrophoresis. *J. Immunol. Methods* **126:** 109-117.

Loppnow, H., Brade, H., Durrbaum, I., Dinarello, C. A., Kusumoto, S., Rietschel, E. T., and Flad, H. D. (1989) IL-1 induction-capacity of defined lipopolysaccharide partial structures. *J. Immunol.* **142:** 3229-3238.

Miyake, K. (2004) Innate recognition of lipopolysaccharide by Toll-like receptor 4-MD-2. *Trends Microbiol.* **12:** 186-192.

Otwinowski, Z., and Minor, W. (1997) Processing of X-ray Diffraction Data Collected in Oscillation Mode. *Methods Enzymol.* **276:** 307-326.

Patterson, B. W., Zhao, G., Elias, N., Hachey, D. L., and Klein, S. (1999) Validation of a new procedure to determine plasma fatty acid concentration and isotopic enrichment. *J. Lipid Res.* **40:** 2118-2124.

Pautsch, A., Vogt, J., Model, K., Siebold, C., and Schulz, G. E. (1999) Strategy for membrane protein crystallization exemplified with OmpA and OmpX. *Proteins* **34:** 167-172.

Perrakis, A., Harkiolaki, M., Wilson, K. S., and Lamzin, V. S. (2001) ARP/wARP and molecular replacement.

Acta. Crystallogr. D **57:** 1445-1450.

Perrakis, A., Sixma, T. K., Wilson, K. S., and Lamzin, V. S. (1997) wARP: improvement and extension of crystallographic phases by weighted averaging of multiple-refined dummy atomic models. *Acta. Crystallogr D* **53:** 448-455.

Raetz, C. R. H., and Whitfield, C. (2002) Lipopolysaccharide endotoxins. *Annu. Rev. Biochem.* **71:** 635-700.

Sambrook, J., Fritsch, E. F., and Maniatis, T. (1989) in *Molecular Cloning: A Laboratory Manual*. 2nd Ed., pp. 1.82-1.84, Cold Spring Harbour Laboratory Press, Cold Spring Harbour (NY).

Schneider, T. R., and Sheldrick, G. M. (2002) Substructure solution with SHELXD. *Acta. Crystallogr. D* **58:** 1772-1779.

Schulz, G. E. (2000) beta-Barrel membrane proteins. *Curr. Opin. Struct. Biol.* **10:** 443-447.

Snijder, H. J., Ubarretxena-Belandia, I., Blaauw, M., Kalk, K. H., Verheij, H. M., Egmond, M. R., Dekker, N., and Dijkstra, B. W. (1999) Structural evidence for dimerization-regulated activation of an integral membrane phospholipase. *Nature* **401:** 717-721.

Steeghs, L., Berns, M., ten Hove, J., de Jong, A., Roholl, P., van Alphen, L., Tommassen, J., and van der Ley, P. (2002) Expression of foreign LpxA acyltransferases in *Neisseria meningitidis* results in modified lipid A with reduced toxicity and retained adjuvant activity. *Cell. Microbiol.* **4:** 599-611.

Storoni, L. C., McCoy, A. J., and Read, R. J. (2004) Likelihood-enhanced fast rotation functions. *Acta. Crystallogr. D* **60:** 432-438.

Terwilliger, T. C. (2003) SOLVE and RESOLVE: automated structure solution and density modification. *Methods Enzymol.* **374:** 22-37.

Trent, M. S. (2004) Biosynthesis, transport, and modification of lipid A. *Biochem. Cell Biol.* 82: 71-86.

Trent, M. S., Pabich, W., Raetz, C. R. H., and Miller, S. I. (2001) A PhoP/PhoQ-induced Lipase (PagL) that catalyzes 3-O-deacylation of lipid A precursors in membranes of *Salmonella typhimurium*. *J. Biol. Chem.* **276:** 9083-9092.

Tsai, C. M., and Frasch, C. E. (1982) A sensitive silver stain for detecting lipopolysaccharides in polyacrylamide gels. *Anal. Biochem.* **119:** 115-119.

Vandeputte-Rutten, L., Bos, M. P., Tommassen, J., and Gros, P. (2003) Crystal structure of Neisserial surface protein A (NspA), a conserved outer membrane protein with vaccine potential. *J. Biol. Chem.* **278:** 24825-24830.

Weeks, C. M., and Miller, R. (1999) Optimizing Shake-and-Bake for proteins. *Acta. Crystallogr. D* **55:** 492-500.

Wimley, W. C. (2002) Toward genomic identification of beta-barrel membrane proteins: composition and architecture of known structures. *Protein Sci.* **11:** 301-312.

Winkler, K. C., and de Haan, P. G. (1948) On the action of sulfanilamide. XII. A set of non-competitive sulfanilamide antagonists for *Escherichia coli*. *Arch. Biochim.* **18:** 97–107.

Winn, M. D., Isupov, M. N., and Murshudov, G. N. (2001) Use of TLS parameters to model anisotropic displacements in macromolecular refinement. *Acta. Crystallogr. D* **57:** 122-133.